Supporting Information for "Trends of hydroclimatic intensity in Colombia"

Oscar Mesa[1] *, Viviana Urrea[1] † and Andrés Ochoa[1] ‡

[1]Departamento de Geociencias y Medio Ambiente, Universidad Nacional de Colombia

Contents of this file

1. Figures S1 to S12

---

*Departamento de Geociencias y Medio Ambiente, Universidad Nacional de Colombia, Carrera 80 # 64-223, 050041 Medellín, Colombia

†Departamento de Geociencias y Medio Ambiente, Universidad Nacional de Colombia, Carrera 80 # 64-223, 050041 Medellín, Colombia

‡Departamento de Geociencias y Medio Ambiente, Universidad Nacional de Colombia, Carrera 80 # 64-223, 050041 Medellín, Colombia

2. Tables S1 to S3

Introduction We analyzed precipitation data both from rain gauges and the CHIRPS database. The gauges are in 1706 sites in the whole territory of Colombia from Colombian Meteorological Service (IDEAM) rain gauge network. Data comprise daily time series of rainfall amounts. We also used the Climate Hazards Group InfraRed Precipitation with Station data (CHIRPS) (Funk et al., 2015).

Figure S1 presents a map of the mean annual precipitation over Colombia. Similar maps for the averages of the other variables considered in this study are in figures S2 to S6. Figure S7 shows the histograms of the spatial distribution of the mean annual precipitation and the mean annual number of rainy days.

Table S1 presents the confusion matrix that illustrates the need to consider the auto-correlation of the series in estimating trends for the variables of this study.

Table S2 shows a sensibility analysis of the results obtained using the different filters of the rain gauge data.

Table S3 presents a regional summary of the trends of the main variables studied.

Figure S8 shows examples of trend analysis for two stations. Figure S9 presents the histograms of the HYINT, INT, and DSL trend slopes. Similarly, Figure S11 presents the trend slope of the histograms of the total annual precipitation, the number of wet days in the year, and the number of wet spells. Figure S10 shows a dispersion diagram of the DSL trend slope vs. INT trend slope. Figures S12 and S13 present maps of the trend slope for the number of wet days, the number of wet runs, the average length of wet runs, and the maximum length of wet runs.

References

Funk, C., Peterson, P., Landsfeld, M., Pedreros, D., Verdin, J., Shukla, S., ... Michaelsen, J. (2015). The climate hazards infrared precipitation with stations—a new environmental record for monitoring extremes. *Scientific Data*, *2*. doi: 10.1038/sdata.2015.66

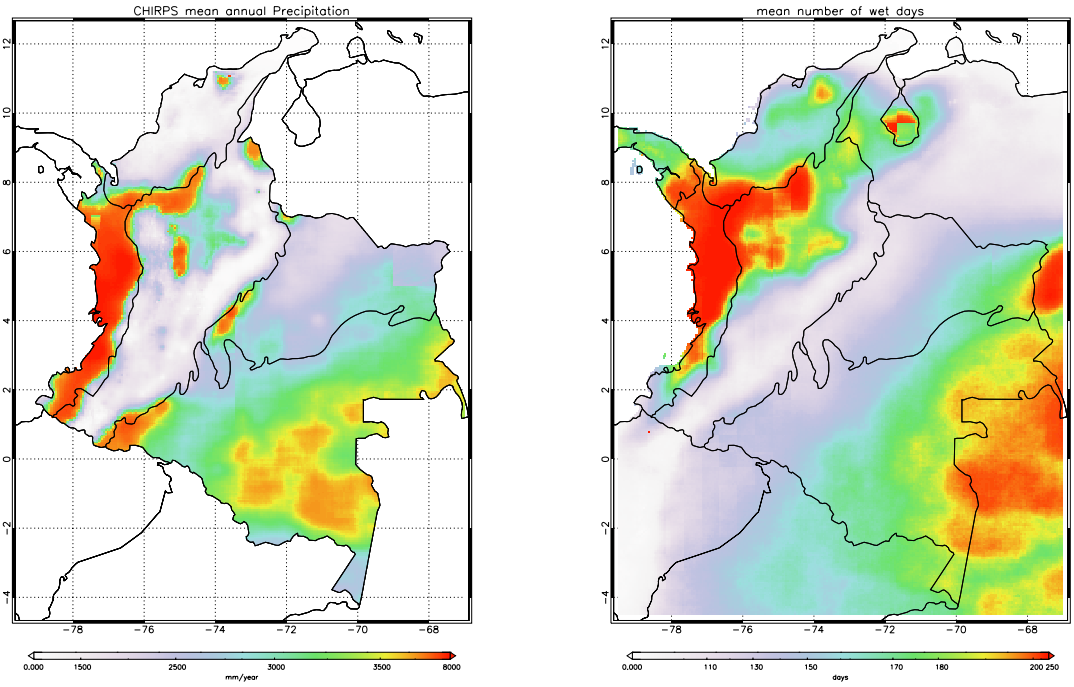

Figure S1. Mean annual precipitation over the period 1981-2018 from CHIRPS database (left). Mean annual number of rainy days over the same period (right).

Table S1. Confusion matrices for the evaluation method of the significance of the trends for each of the indicated variables without taking into account auto-correlation. For the illustration, the Mann-Kendall test with auto-correlation is considered the true one. The Table shows the results for the fourth sensibility data set, but notice the similarity among all datasets.

Variable	true trend R-R	false trend R-NR	false no trend NR-R	true no trend NR-NR
	Number of gauges (Percentage of the total number of gauges)			
P	45 (3%)	293 (18%)	180 (11%)	1111 (68%)
INT	116 (7%)	400 (25%)	245 (15%)	868 (53%)
DSL	62 (4%)	316 (19%)	184 (11%)	1067 (66%)
HY-INT	108 (7%)	393 (24%)	212 (13%)	916 (56%)

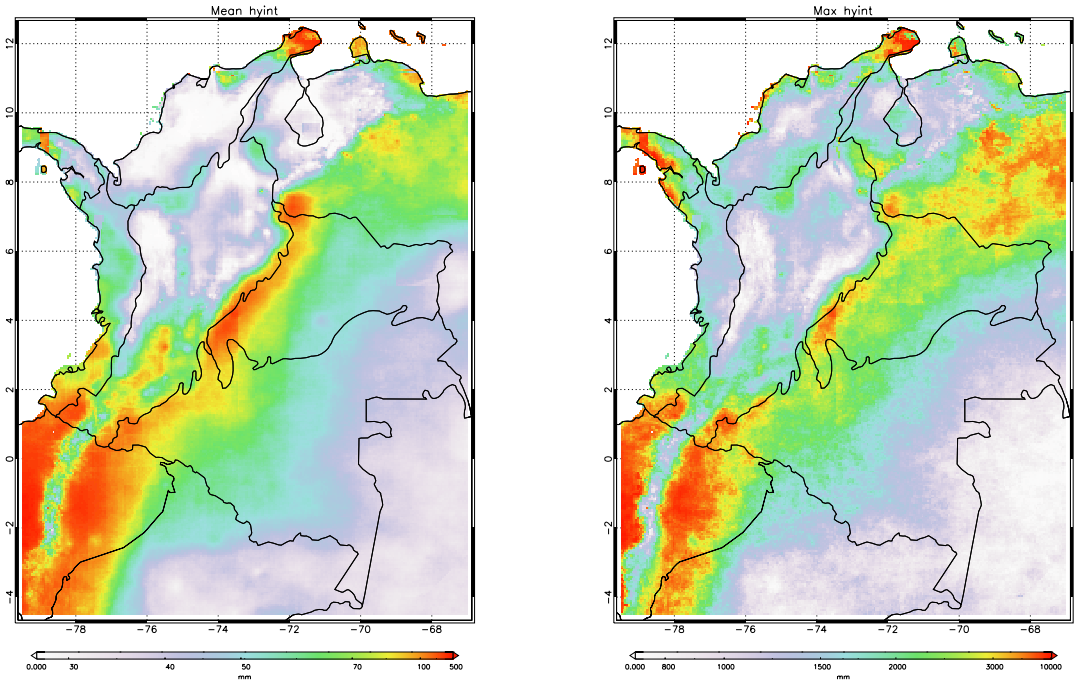

Figure S2. Average hyint over the period 1981-2018 from CHIRPS database (left). Average hyintx over the same period (right).

Table S2. Comparison of sensibility alternatives for data filtering. Percentage of stations with a significant trend for each of the four sensibility data sets (%S1 to %S4) and percentage of those with positive trends (%P1 to %P4). Variable symbols are the same as in Table 1.

Variable	%S1	%S2	%S3	%S4	%P1	%P2	%P3	%P4
N Gauges	355	1345	1320	1629				
P	12	13	14	14	80	81	82	73
INT	21	20	19	22	49	56	59	57
DSL	18	16	15	15	17	18	20	31
HY-INT	22	18	18	20	29	33	34	40
N Wet Days	18	17	17	17	74	81	80	71
WSL	20	19	17	18	83	75	74	64
N Wet Runs	17	15	14	14	66	64	62	58
INTX	11	9	10	9	68	62	64	57
DSLX	11	9	10	9	34	27	26	20
HYINTX	10	9	10	9	43	34	37	26
WSLX	17	14	14	14	77	74	71	64

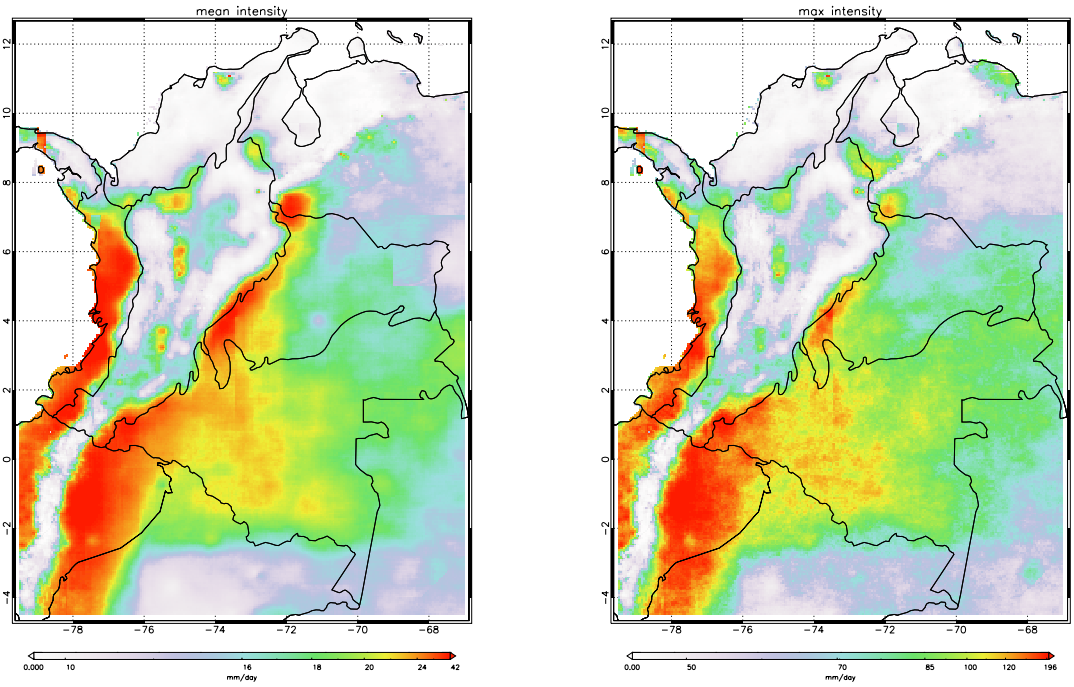

Figure S3. Mean average intensity over the period 1981-2018 from CHIRPS database (left). Mean maximum intensity over the same period (right).

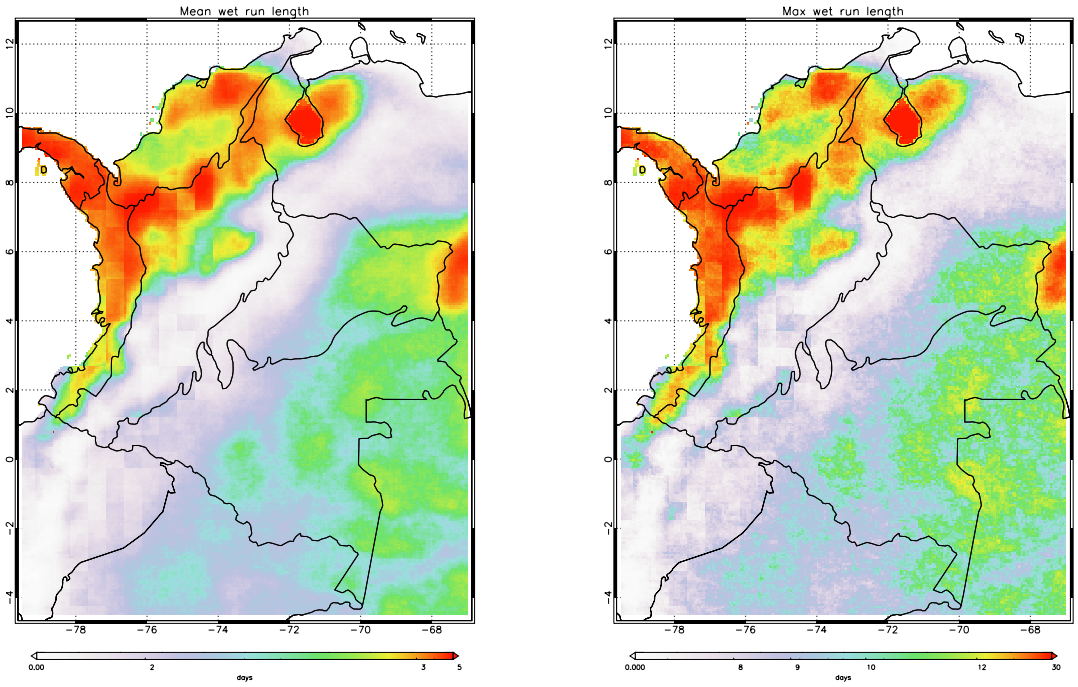

Figure S4. Mean wet run length over the period 1981-2018 from CHIRPS database (left). Mean maximum wet run length over the same period (right).

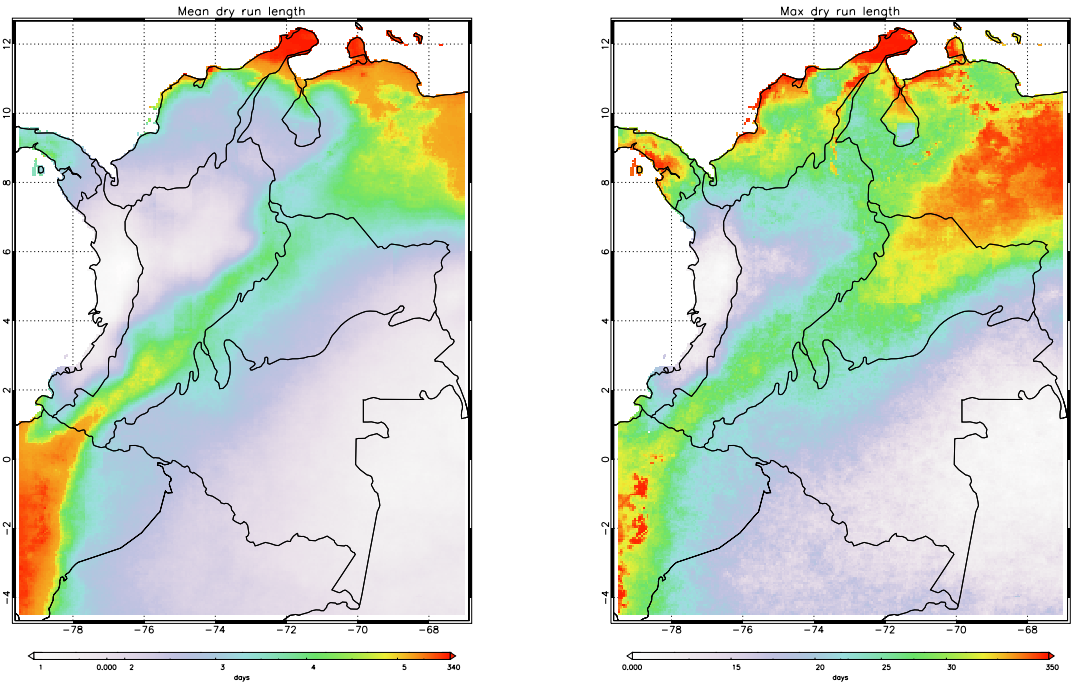

Figure S5. Mean dry run length over the period 1981-2018 from CHIRPS database (left). Mean maximum dry run length over the same period (right).

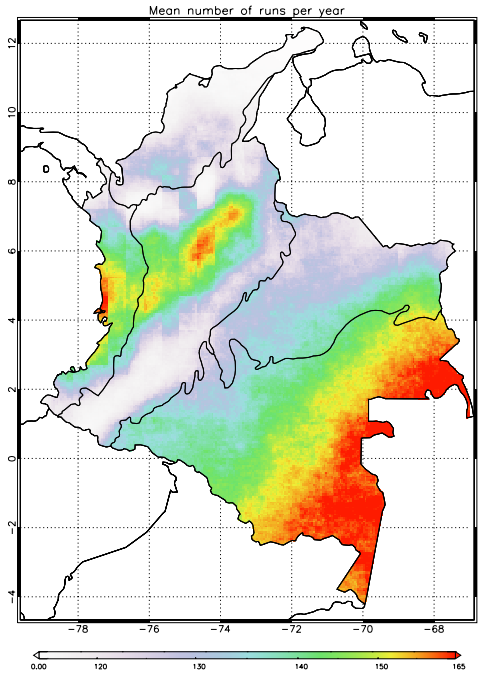

Figure S6. Mean number of runs over the period 1981-2018 from CHIRPS database

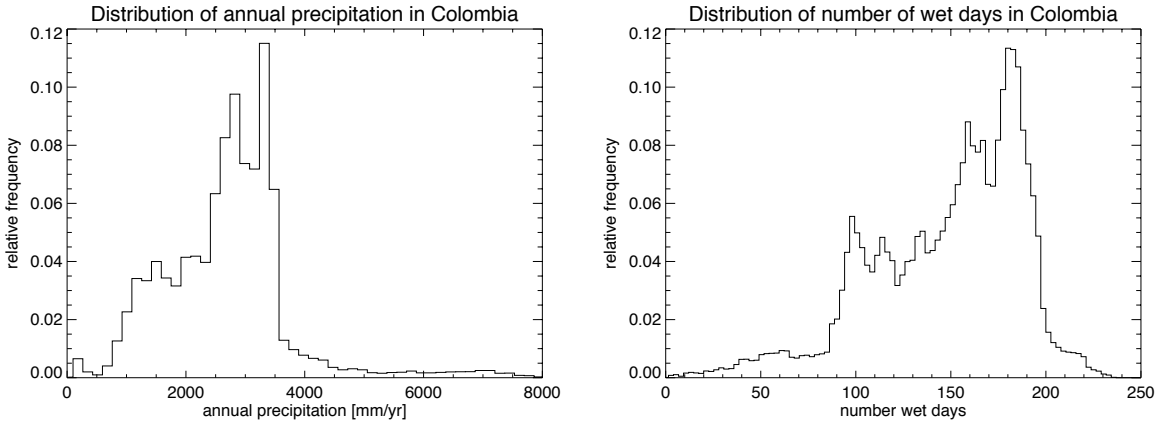

Figure S7. Histograms of mean annual precipitation over the period 1981-2018 from CHIRPS database (left) and mean annual number of rainy days over the same period (right).

Table S3. Regional summary of the trends of the base rain gauges and CHIRPS datasets for Total Annual Precipitation, HY-INT, INTX and HYINTX. Column symbols as in Table 1. The number of stations and pixels for each region are: Amazon, 12 and 14006; Andes, 622 and 9741; Caribbean, 207 and 3901; Orinoco, 30 and 6729; and Pacific, 38 and 2635 respectively

	Rain Gauges		CHIRPS	
Region	% Rej/T	% Pos/Rej	% Rej/T	% Pos/Rej
	Total Annual Precipitation			
Amazon	0	-NaN	10	80
Andes	12	73	6	84
Caribbean	14	90	4	97
Orinoco	17	80	8	50
Pacific	24	100	28	76
Total	13	79	10	76
	HY-INT			
Amazon	25	0	12	0
Andes	20	30	31	79
Caribbean	21	36	40	4
Orinoco	17	60	22	0
Pacific	37	43	31	100
Total	21	33	23	38
	INTX			
Amazon	17	0	4	43
Andes	11	62	20	53
Caribbean	8	62	22	5
Orinoco	7	100	12	12
Pacific	8	67	17	100
Total	10	62	13	40
	HYINTX			
Amazon	8	0	5	17
Andes	10	38	13	71
Caribbean	6	58	12	26
Orinoco	7	100	6	3
Pacific	24	0	15	100
Total	10	38	9	48

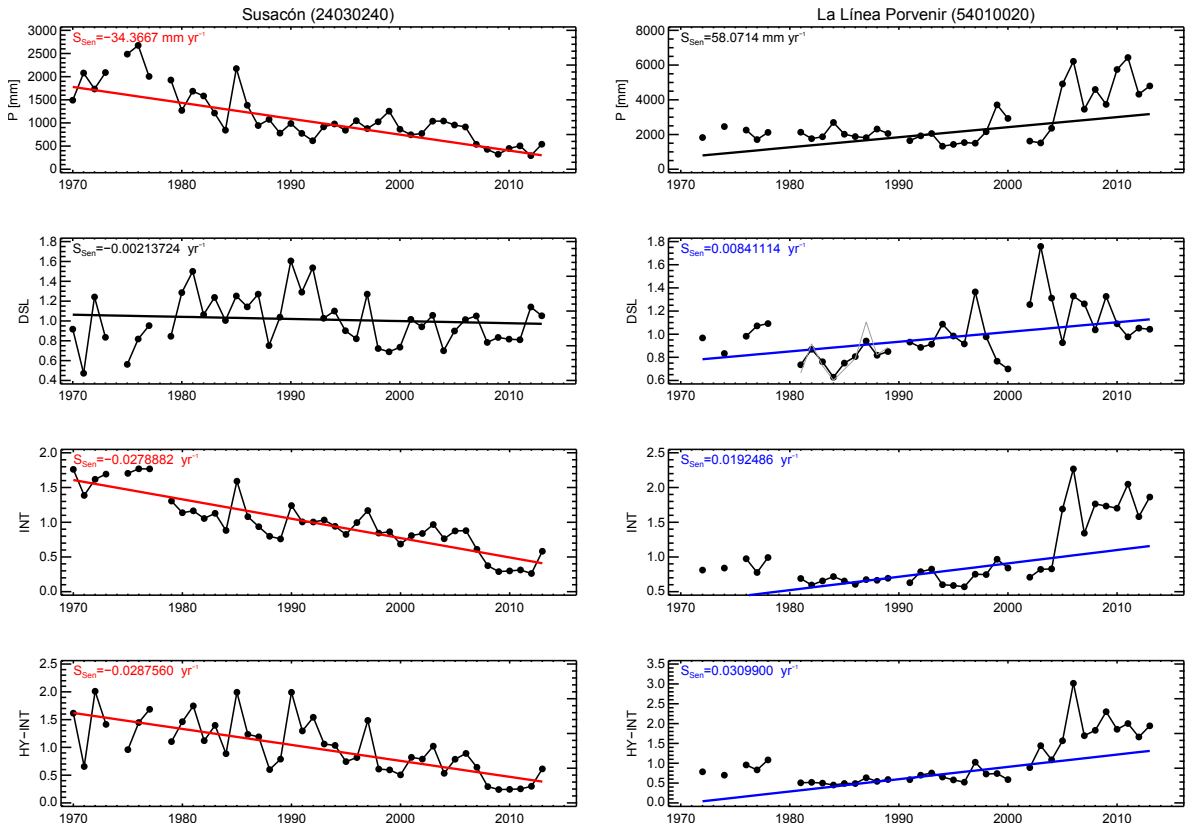

Figure S8. Two examples of trend analysis for (top to bottom) P, DSL, INT, and HY-INT for two representative stations, left panel: Susacón in Boyacá, at 2550 masl, right panel: La Línea El Porvenir in Risaralda, at 1955 masl.

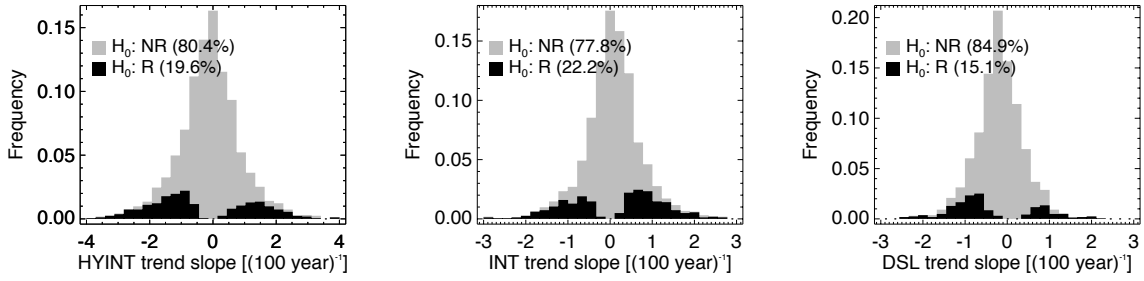

Figure S9. Histograms of the HYINT (left), INT (center), and DSL (right) trend slopes of the fourth alternative dataset. Non-significant trends (H_0: Stationary hypothesis not rejected, NR) in grey and significant trends in black (H_0: Stationary hypothesis rejected, R). Results are similar for other datasets.

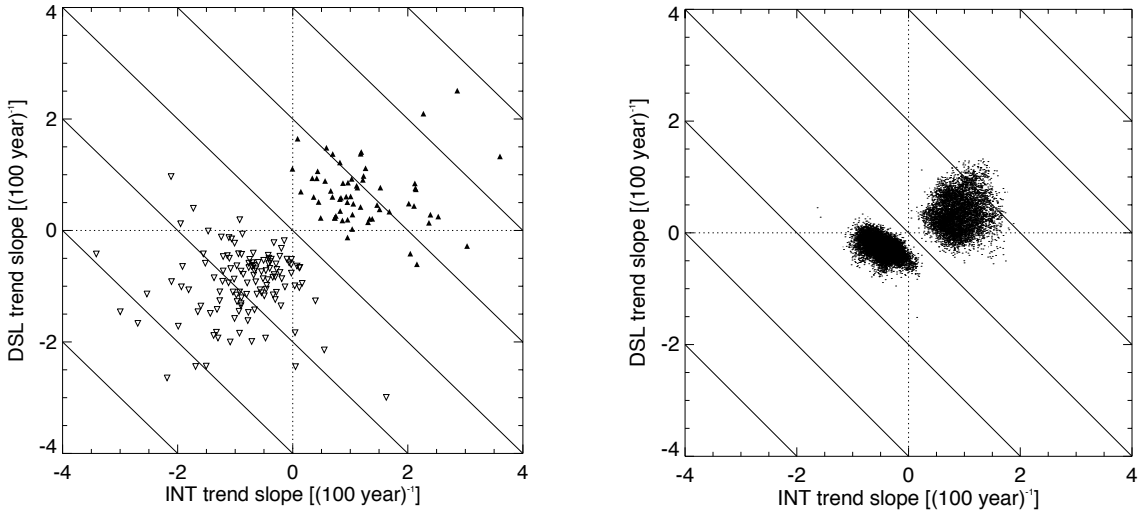

Figure S10. Dispersion diagram of the DSL trend slope vs. INT trend slope for all stations in the base dataset (left) and all pixels in the chirps dataset (right) with significant HY-INT trend slope. Notice that because of Eq 10, the trend slope of HY-INT is the sum of the trend slopes of INT and DSL. This equation explains the slanted iso-lines for the HY-INT trend slope.

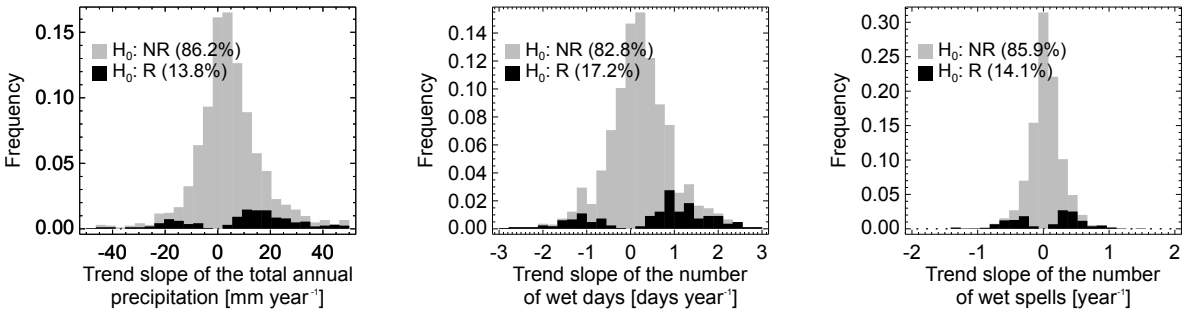

Figure S11. Same as Figure S9 for the trend slope of the total annual precipitation (left), the number of wet days in the year(center) and number of wet spells in the year (right).

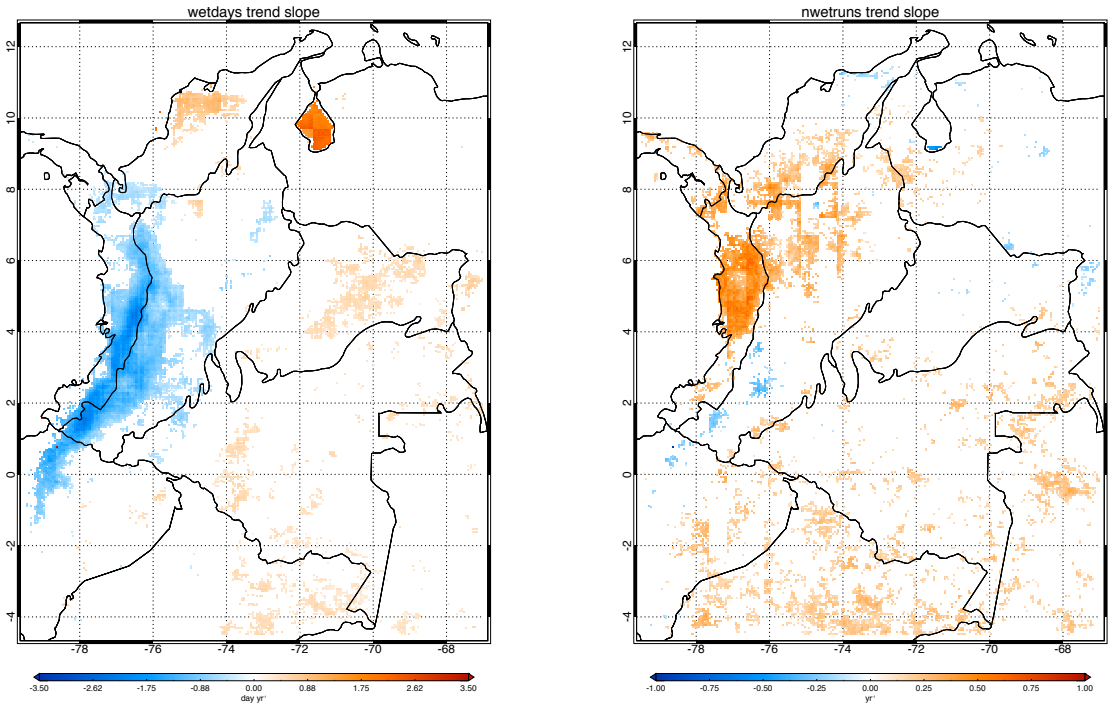

Figure S12. Maps of the trend slope for number of wet days (left) and the number of wet runs (right) for CHIRPS data set. No significant trends are not plotted.

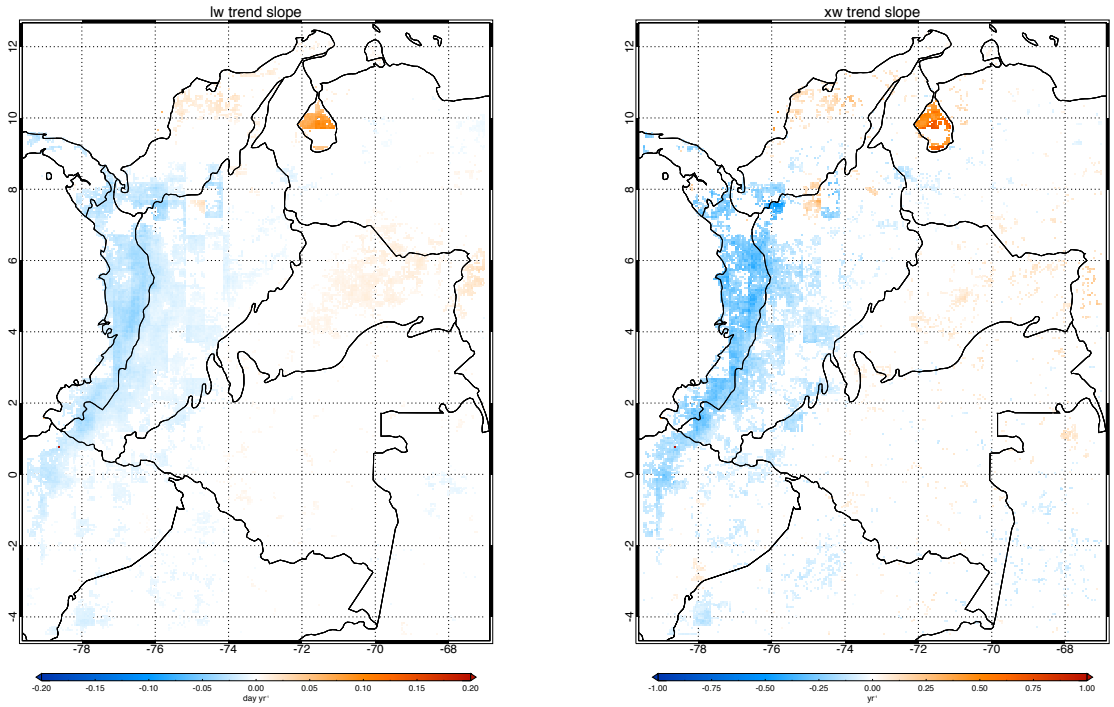

Figure S13. Maps of the trend slope for average length of wet runs (left) and the maximum length of wet runs (right) for CHIRPS data set. No significant trends are not plotted.